Spectroscopy of Light Echoes from η Carinae's 19th-Century Great Eruption

A. Rest[1], J. L. Prieto[2,3], N. R. Walborn[1], N. Smith[4], F. B. Bianco[5,6], R. Chornock[7], D. L. Welch[8], D. A. Howell[5,6], M. E. Huber[9], R. J. Foley[7,10], W. Fong[7], B. Sinnott[8], H. E. Bond[1], R. C. Smith[11], I. Toledo[12], D. Minniti[13], K. Mandel[7,14]

[1]*Space Telescope Science Institute, 3700 San Martin Dr., Baltimore, MD 21218, USA*
[2]*Carnegie Observatories, 813 Santa Barbara Street, Pasadena, CA 91101, USA*
[3]*Hubble, Carnegie-Princeton Fellow*
[4]*Steward Observatory, University of Arizona, 933 North Cherry Avenue, Tucson, AZ 85721, USA*
[5]*Las Cumbres Observatory Global Telescope Network, Goleta, CA 93117, USA*
[6]*Department of Physics, University of California, Santa Barbara, CA 93106, USA*
[7]*Harvard-Smithsonian Center for Astrophysics, 60 Garden Street, Cambridge, MA 02138, USA*
[8]*Department of Physics and Astronomy, McMaster University, Hamilton, Ontario, L8S 4M1, Canada*
[9]*Department of Physics and Astronomy, Johns Hopkins University, Baltimore, 3400 North Charles Street, MD 21218, USA*
[10]*Clay Fellow*
[11]*Cerro Tololo Inter-American Observatory, National Optical Astronomy Observatory, Colina el Pino S/N, La Serena, Chile*
[12]*ALMA, KM 121 CH 23, San Pedro de Atacama, II Region, Chile*
[13]*Dept. of Astronomy and Astrophysics, Pontifica Universidad Catolica, Santiago 22, Chile*
[14]*Imperial College London, Blackett Laboratory, Prince Consort Rd, London SW7 2AZ, UK*

η Carinae (η Car) is the most massive star known in the Milky Way[1], and a prototype of the poorly understood Luminous Blue Variable stars. It is in a binary system with a period of 5.52 years[2]. Since it is one of the few systems close enough (2.3 kpc) to resolve circumstellar material and has evolved on a human timescale, much of our knowledge about the mass loss of massive stars is derived from this system[3]. It became the second-brightest star in the sky during its mid-19th century "Great Eruption," but then faded from view; only visual estimates of its brightness were recorded and nothing is known about the eruption's spectrum[4]. Here we report the discovery of light echoes of η Car which appear to be from the 1838-1858 eruption. While some of the light from the eruption traveled directly to Earth and was observed in the mid-19th century, light directed away from the Earth scattered off a dust sheet and has now been observed after a half-century delay. Spectra of these light echoes provide a direct estimate of the effective temperature and other physical properties of this eruption including the expansion speed, raising questions about traditional scenarios for the eruption that involve a minimum temperature for steady opaque winds. We also find important differences between the light-echo spectra of η Car and spectra of extragalactic transients previously presumed to be analogues.

Because of its proximity, η Car is probably the most intensely scrutinized massive star system. It lies at the heart of the Carina star-forming region, is surrounded by an intricate circumstellar nebula ejected during the Great Eruption, has spectacular variability at all wavelengths[1], and is in a binary system with a period of 5.52 years [2]. The Great Eruption is thought to have ejected more than 10 $M_{\odot}$ from the star, and to have released about 10% of the energy of a core-collapse supernova (SN)[5,6], even though the star survived the event. The underlying physical mechanism of the outburst remains unexplained.

Some extragalactic non-SN transients have been interpreted as analogues of the Great Eruption of η Car [7–12]. However, their widening diversity calls into question their association or suggests that massive eruptions like η Car are only a subset of non-terminal eruptions[13]. An important gap in our understanding is that until now we have had only visual brightness estimates for the Great Eruption of η Car[4], whereas we have modern spectra and precise photometry for the extragalactic transients.

1 Light Echoes of η Carinae's Great Outburst

In 2003, 2010, and 2011, we obtained images with the CTIO 4-m Blanco telescope of a region $\sim$0.5 degrees to the south of η Car (Figure 1) that, when differenced, show a rich set of light echoes. We have also found similar echo candidates at other positions, which we are currently monitoring. Applying the vector method that previously allowed us to identify the source of the light echoes from the SNe that produced the SNRs 0509$-$67.5, Cas A, and Tycho[14,15], we find that a dramatic brightening of η Car must be the origin. In these echoes, unlike those of Galactic SNe[16], there is still significant spatial overlap even at separations of one light-year, suggesting that the duration of the event causing them must be significantly longer than one year. We also see brightening of 2 magnitudes or more within 8 years. Thus, the Lesser Eruption from 1887 to 1896, which brightened by only a magnitude, is excluded as the source. The large brightening and long duration point to the Great Eruption as the source of the light echoes.

We have also obtained a composite light curve in the SDSS i filter of the light echoes from other telescopes (see Fig. 2), showing a slow decline of several tenths of a magnitude over half a year. Within the Great Eruption there are three known peaks[4] at 1838, 1843, and 1845. The echo light curve is most consistent with the historical observations of the 1843 event, although further observations are necessary to be certain (see the Supplementary Information, SI).

2 Spectroscopy

Three spectra of the light echo are shown in Figure 3 — the positions differ only slightly in slit angle (see Table S1). The light-echo spectra do not show emission lines, only absorption lines characteristic of cool stellar photospheres. In particular, the Ca II infrared (IR) triplet is in absorp-

tion and not in emission. The right panel of Figure 3 shows the region of Hα and [N II]. Because of bright ambient nebular emission, it is difficult to determine if there is any emission from η Car itself, but in any case it must be weak if present. By cross-correlating each of our η Car echo spectra with the UVES spectral library[17] (see Figure S6 and S7) we find best agreement with supergiant spectral types in the range of G2-G5, with an effective temperature of $\sim$5000 K. Spectral types of F7 or earlier are ruled out by our analysis (see SI for more details).

The Ca II IR triplet absorption features in the spectrum are noticeably blueshifted (see Figure S6). By cross-correlation with G-type[18] templates, we determine velocities of -202 ± 9, -210 ± 14, and -237 ± 17 km s^{-1} for our three spectra. Averaging these, and adding an uncertainty for the the motion of the scattering dust sheet, we estimate the average velocity to be -210 ± 30 km s^{-1}.

The bipolar nature of Homunculus Nebula shows that the η Car Great Eruption was strongly aspherical. It was previously predicted that the outflow speeds one would derive from spectra of η Car in outburst, looking at the poles and equator of the double lobes, would be ~ -650 km s^{-1} and -40-100 km s^{-1}, respectively[3] (outflow speeds near the equator have a steep latitude dependence). The light echo we investigate in this paper arises from latitudes near the equator of η Car (see Figure S5), and the measured blue-shifted velocity of -210 ± 30 km s^{-1} is in good agreement with expansion speeds within $\pm 20^{\circ}$ of the equatorial plane. We also find a strong asymmetry in the Ca II IR triplet, extending to a velocity of -850 km s^{-1}. This is well below the speeds of the fastest polar ejecta found previously[6], but is in good agreement with speeds observed in the blast wave at lower latitudes[6]. Future observations of light echoes viewing the η Car eruption from different directions, in particular from the poles, may have the potential to observe these very high-velocity ejecta and other asymmetries.

3 Comparison to LBVs and SN impostors

Luminous Blue Variable (LBV) outbursts are divided into two classes[8,11,19]: "S Doradus (S Dor)-like" excursions in the HR diagram from OB to AF spectral types, with changes in the visual brightness of 1-3 magnitudes but nearly constant bolometric luminosity, and η Car-like giant eruptions with the brightness increasing visually by more than 3 magnitudes, an increase in the bolometric luminosity, and an increase in the mass-loss rate[8,9]. A characteristic of both types of LBV outbursts is their transition from a hot quiescent state to a cooler outburst state, although this feature is less well observed for the giant eruptions (see Figure 4).

While neither type of LBV outburst is well understood, the traditional mechanism for η Car-like giant eruptions is an unexplained increase in luminosity that drives a denser wind, so that an optically thick pseudo-photosphere forms at a layer much larger and cooler than the hydrostatic stellar surface. As the mass-loss rate increases, the effective temperature decreases and the effective photosphere of the star moves outward into the wind[20]. This scenario predicts a minimum

effective temperature of $\sim$7000 K (an F-type spectrum) due to the temperature dependence of the wind opacity. In contrast, S Dor-type outbursts are suggested to involve an actual expansion of the stellar photospheric radius; these events also have minimum temperatures in the 7000-9000 K range and exhibit spectra at maximum resembling A or F-type supergiants[8,19]. These events evidently occur as a massive star attempts to evolve redward and encounters the Humphreys-Davidson Limit, beyond which no stable stars are observed.

Surprisingly, our G-type light-echo spectrum of the η Car Great Eruption is inconsistent with expectations of an opaque-wind model[20] (see Figure 4). This model also fails to explain the high 10^{50} erg kinetic energy[5] and the presence of a fast blast wave at large radii[6]. Instead, these observations point toward a hydrodynamic explosion mechanism[2,5,6]. Other alternative models involving accretion in a binary system have also been proposed[12].

The first *visual* spectroscopic observations of η Car around 1870 showed emission lines [21,22]. A photographic spectrogram obtained during its Lesser Eruption circa 1890[23,24] resembles an F-type supergiant blueshifted by -200 km s^{-1}, with moderate hydrogen P Cygni profiles, which *is* as expected in the opaque-wind model[20]. The difference between the 1890 and our light-echo spectra of the Great Eruption is therefore quite striking, indicating that two distinct physical processes may have been involved. However, the 1890 event also produced a mass ejection, the Little Homunculus, with the same axial symmetry as the Great Eruption[25], albeit of a much smaller amount.

Although η Car's Great Eruption has been considered the prototype of the so-called SN impostors or η Car analogues, it is actually an extreme case in terms of radiated energy ($10^{49.3}$ erg), kinetic energy ($>10^{50}$ erg), and its decade-long duration[13]. Typically, the hotter SN impostors have steep blue continua, stronger and broader Balmer lines, and relatively weak absorption, whereas the cooler ones tend to have redder continua, weaker and narrower Balmer lines, strong [Ca II] and Ca II emission, deeper P Cygni absorption features, and in some cases stronger absorption spectra similar to F-type supergiants[13]. However, the η Car Great-Eruption light-echo spectrum is quite different. Its spectral type is G2-G5, significantly later than all other SN impostors at peak. Furthermore, the Ca II IR triplet lines are only in absorption. It is difficult to see how strong emission lines could be avoided in an opaque wind where the continuum photosphere is determined by a change in opacity, so this is another argument against that model. For the extreme mass-loss rates required in η Car's Great Eruption, another process must give rise to the apparent temperature.

The Great Eruption of η Car is one of the most spectacular known astronomical events, providing valuable clues for understanding massive stars, stellar mass loss, LBVs, and SN impostors. Yet for a century and a half we were missing critical spectral information about the eruption itself, due to the technological limitations of the past. The discovery of its light echoes gives us a second chance to relive this important event. The early data presented here have already revealed surprises. Many more will come as we continue to watch echoes from the Great Eruption in real

time, as we follow new echoes from different time periods, and as we add spatial information to build a four-dimensional picture of the death throes of one of the most interesting objects in the Milky Way.

Acknowledgements We thank R. Humphreys, K. Davidson, and J. Vink for comments and discussions. We thank S. Blondin for help with the continuum subtraction. The Blanco 4m telescope is a facility of the Cerro Tololo Inter-American Observatory, National Optical Astronomy Observatory, which are operated by the Association of Universities for Research in Astronomy, under contract with the National Science Foundation. We use data from the UVES Paranal Observatory Project. The computations in this paper were run on the Odyssey cluster supported by the FAS Science Division Research Computing Group at Harvard University. Observations were obtained at LCOGT, and FBB and DAH acknowledge support from LCOGT.

Author Contributions All authors contributed to the drafting of the paper. A.R., N.S and R.C.S. imaged the area around η Car. A.R. and M.H. reduced the imaging data. H.E.B. provided images of the echoes that guided our spectroscopic pointings. J.L.P., R.C., R.J.F., and W.F. obtained the spectra and reduced them. A.R. and J.P.L. performed spectral analysis and interpretation. A.R., N.R.W., and F.B.B performed spectral classification. F.B.B. and K.M. correlated the spectra. A.R., D.L.W. and B.S. modelled the light echo. I.T. and D.M. provided imaging of η Car. F.B.B and D.A.H provided the FTS images, F.B.B and A.R. reduced them.

Author Information The authors declare that they have no competing financial interests. Correspondence and requests for materials should be addressed to A.R. (arest@stsci.edu).

S4 Supplemental Information

Three dimensional orientation The scattered-light path is shown in Figure S5. The 3D-plot shows that with this light echo we see the eruption of η Car from a viewing angle perpendicular to the principal axis of the Homunculus Nebula. It will be very interesting to compare spectra seen from this viewing angle with spectra from light echoes that view the eruption from the poles of the bipolar outflow.

Evidence that these are light echoes of the mid-19th century Great Eruption of η Car The angular separation between the center of our light-echo images and η Car is $\sim$0.5 degrees, as shown in the left panel of Figure 1, in which our pointing is indicated with a white box. In the middle panel of this figure, our three epochs of SDSS *i*-band imaging obtained with the $8\mathrm{k} \times 8\mathrm{k}$ Mosaic imager on the CTIO 4-m Blanco telescope are displayed. The images, each with an exposure of 160 s, were obtained on 2003 Mar 10 (*A*), 2010 May 10 (*B*), and 2011 Feb 6 (*C*). Difference images, $C - A$ and $C - B$, are also shown (upper and middle right panels, respectively). In them, we notice excess flux from the first (black) and second epochs (white), which we interpret as light echoes from η Car. Sample light-echo positions are indicated with blue (epoch *A*) and red (epoch *B* and *C*) arrows.

Comparing the first- and second-epoch images, we can determine the direction of the apparent motion of the light echo and infer the direction to the illuminating source. Most of the excess flux in the first-epoch image is toward the northern part of the image (blue arrows in Figure 1, whereas most of the excess flux in the second-epoch image is in the southern portion (red arrows in Figure 1. If the light echoes arise from η Car, this is exactly the directional sense expected. We have also found similar regions of excess flux at other positions in proximity to η Car, with apparent motions consistent with η Car being the source of the outburst light, which we will discuss in a follow-up paper. The vector method we have used previously to determine the origin of the light echoes for SNR 0509$-$67.5, Cas A, and Tycho[14,15] was applied here and, not surprisingly, we conclude that these excess fluxes are most likely light echoes from a dramatic brightening of η Car.

The flux profile of a light echo, which is the cut through the light echo along the axis pointing toward the source event, is the projected light curve, stretched or compressed depending on the inclination of the scattering dust filament, and convolved with the effects of the dust width and the seeing[16]. In pathological cases where the inclination of the dust filament is very unfavorable or where the dust filament is significantly thicker than any yet observed, a useful correspondence may be lost[16]. For light echoes from sources in our Galaxy scattered by dust with typical widths and inclinations, we expect that the apparent motion of the light echo will move at a rate of one projected echo width between two epochs separated by twice the outburst event duration. For known galactic SNe light echoes the timescale of the brightest phase is of the order of a few months, so that an imaging separation time of 1 year is sufficient for there to be no overlap (on

the sky) of light-echo features[14,15]. For a several-decade duration outburst, like that of η Car, the difference image $C-B$ has only a time difference of 1 year, and can only reveal the small boundary fractions of the light echo in C, whose more complete extent can be seen in $C-A$ which has a time difference of 8 years. We conclude that the duration of the event illuminating these light echoes is significantly longer than one year, consistent with our conclusion that these are echoes of the 20-year long Great Eruption of η Car.

Determination of spectral type We compare the light-echo spectra to the compilation of supergiant spectra in the UVES atlas[17] (see Table S2). The upper left panel of Figure S6 shows the light-echo spectra, flattened by dividing by low-order continuum fits, and the UVES supergiant sequence. The instrument configuration for the EC1A spectrum was designed to optimize the S/N ratio in the wavelength region of the Ca II IR triplet, resulting in a lower S/N ratio for $\lambda < 6000$ Å. For this reason the EC1A spectrum is absent from the upper left panel of Figure S6. The light-echo spectra correlate very well with late-F and G-type stars, in particular the Mg b lines and line blends at 5270 Å and 6497 Å. Both earlier- and later-type spectra show significantly fewer similarities.

We calculate the cross-correlation parameter r between the light echo and the UVES spectra using the IRAF routine `xcsao` in the wavelength range 5050-6500 Å (see left panel of Figure S7). We exclude wavelength ranges contaminated by fore/background emission lines (see Table S4). We find that extending the wavelength region to redder wavelengths (e.g., 5050-7500 Å) decreases the correlation, and in particular the correlation differences between the different spectral types. The reasons for a decrease in correlation are threefold: (1) the spectral differences between F, G, and K stars are stronger in the bluer wavelength ranges, and therefore including redder wavelengths dilutes the discrimination power, (2) strong fore/background emission lines like H_α, N II, and S II introduce large discontinuities in the wavelength coverage, and (3) the chip gaps fall into the 6500-7500 Å wavelength range, further adding to the discontinuities. For the above reasons we determine the 5050-6500 Å wavelength range to be optimal for the correlation analysis.

To quantitatively estimate the temperatures of the supergiants that correlate best, we smooth $r(T_{eff})$ with a Gaussian of width $\sigma = 300$ K (see lines in left panel of Figure S7). We find that the temperature with maximum correlation is 5210 K and 4950K for EC1B and EC1C, respectively. The right panel of Figure S7 shows the probability density functions (PDFs) of the temperature, T_{eff}, of the supergiant spectral template having the best smoothed correlation, $r(T_{eff})$, with each light-echo spectrum. The PDFs are computed by bootstrap resampling of the distribution 10^5 times. The 95% confidence intervals of the best-matching temperatures are 4850-5550 K (spectral type G0-G5) and 4450-5400 K (spectral type G0-K1) for EC1B and EC1C, respectively. Using an extended wavelength range of 5050-7500 Å, the 95% confidence intervals are 3700-6300 K (F8-K5) and 3450-5100 K (G2-M1) for EC1B and EC1C, respectively. For the reasons mentioned above, the extended wavelength range results in a spectral type that is less constrained compared to the 5050-6500 Å range. We conclude that the light-echo spectra agree best with supergiant spectral types in the range of G2-G5, with an effective temperature of $\sim$5000 K. We conservatively exclude spectral types of F7 and earlier.

Unfortunately, the UVES spectra have a gap in coverage around the Ca II IR triplet, and therefore we use a compilation of supergiant spectra[18] covering the Ca II triplet wavelength range (see Table S3). The lower-left panel of Figure S6 compares the observed light-echo spectrum with this atlas. For early-type stars up to G0, the wavelength range redward of 8300 Å is mainly dominated by the H Paschen series, which contaminates the Ca II triplet but gradually disappears as the effective temperature decreases[18]. Note that the observed light-echo spectra do not show any clear signs of the H Paschen lines; in particular, the lines at 8409 Å and 8498 Å are at most very weak. The earliest spectral types in agreement with such weak or non-existent H-Paschen lines are late F-types, in excellent agreement with the spectral correlation results in the wavelength range 5050-6500 Å.

Visual observers noted a reddish or "ruddy" color during η Car's Great Eruption, e.g. described by Herschel as "redder than Arcturus"[4,28]. These observations point to a temperature of $T_{eff} < 4500$ K, lower than the temperature we infer from the spectral lines. It is plausible that reddening by grains forming in the eruption cause the apparent color. We note, however, that the temperature inferred from the spectral type is much more reliable than an apparent color, in particular one done visually, since it is not influenced by reddening due to unknown amounts of new dust formation along the line of sight.

The lower-right panel of Figure S6 shows velocities determined from cross-correlation from spectra of different spectral types. The contribution to the derived velocity due to motion of the reflecting dust sheet, i.e. the *moving-mirror effect*, is likely less than 30 km s^{-1} given the relatively low dominant expansion speeds of cool gas in the Carina Nebula H II region[29]. This systematic error could be constrained better with more spectra of light echoes located close enough to each other that they probe similar viewing angles, but different enough that the scattering dust is parsecs apart and thus has independent velocities.

The most similar SN impostor The closest SN impostor in temperature is UGC 2773 OT2009-1, which is also dominated by a forest of absorption lines, similar to an F-type supergiant[26,27]. However, the Ca II IR triplet has a P Cygni profile with a strong emission component[27]. Interestingly, UGC 2773 OT2009-1 is also one of the few examples where the outburst has persisted for years and in fact still continues[13,26,27].

Hα line The interpretation of the Hα emission line is difficult, since the fore/background emission line subtraction is imperfect. The left panel of Figure 3 shows the Hα line of the three observed light-echo spectra. Both EC1B and EC1C show narrow emission at zero velocity, most likely due to the incompletely subtracted fore/background emission. However, they also show asymmetry at the wavelength for which we would expect Hα emission if the hydrogen has the same blueshifted velocity of -210 km s^{-1}, indicated with the red line. If this is indeed a blueshifted Hα from the eruption, it is a narrow one unlike many of the SN impostors, but similar to the coolest ones like UGC 2773 OT2009-1[26,27] .

Epoch of Spectra The slit position of the light echo spectrum is shown in the bottom right panel of Figure 1. Because the η Car Great Eruption lasted over a decade, it is not straightforward to determine the epochs probed by the light-echo spectra. In order to attempt this, we compare the historical light curve[4] (see Figure 2) with time variation of the light echoes.

We summarize here an account[4] of the photometric history of the Great Eruption of η Car. John Herschel recorded a brightening of $\sim$1 mag in less than two weeks near the end of 1837. Over the next few months, η Car slowly faded again. Unfortunately, there is a gap in brightness estimates for the period between late 1838 and 1841. There was another brightening in early 1843, and then another episode where η Car again faded back to typical non-outburst brightness. Late in 1844, η Car's greatest recorded brightening episode began, with peak brightness occurring in early 1845. Thereafter a slow decline began which lasted for the next decade.

We can compare η Car's historical light curve to the light curve we derived from the light echoes: at a given epoch and position on the sky, the light-echo flux is the flux of the source event integrated over a range of epochs. The range of epochs represented in the instantaneous flux at a given pointing depends on both astrophysical (dust width and inclination) and observational (seeing) factors, and can be represented by a near-Gaussian window function[16]. For the light-echo systems we have characterized around the Cas A and Tycho remnants, the full width at half maximum was on the order of 25-120 days[16]. Thus if the flux at the same spatial position is measured at different epochs, the brightness recorded will be the true outburst light curve convolved with the window function.

With four more epochs of the light echo obtained at the Faulkes Telescope South (FTS) 2-m telescope, we generated light curves of η Car at 17 positions along the spectroscopic slit shown in Figure 1. Since we have images from 2003 to mid-2011, these light curves span $\sim$8 years. After an overall normalization to each of these light curves to match each other, the differences in light-curve profiles are remarkably small, with a typical standard deviation in flux of 2-4% (see Table S5). We therefore average these light curves into a single light curve. We show this light curve in Figure 2, shifted by 174.2 yrs (green circles), 167.95 yrs (red circles), and 166.28 yrs (blue circles) in order to match the 1838, 1843, and 1845 outbursts, respectively. The earliest epoch (2003) needs to be considered an upper limit, since that epoch was used as the template for the difference imaging, and we determined the light-echo flux at that epoch as the difference between the flux in the template image and the flux at a different, apparently empty position in the same image. In other words, there is an undetermined flux zeropoint when an on-frame reference location may contain light echo flux. It is also important to note that the light echo light curve is determined from images in SDSS i, which can introduces systematics when comparing it to the visual magnitude of the historical light curve, in particular since LBV's change their colors during outbursts.

The light-echo light curve we derive from our images clearly reveals brightening of 2 mag-

nitudes or more within an interval of 8 years. The Lesser Eruption of η Car from 1887 to 1896 caused η Car to brighten by roughly 1 magnitude only. Unless the Lesser Eruption was extremely asymmetric such that it increased by an additional 1 magnitude or more in the direction of the light echo, the Lesser Eruption is excluded as the source of the light echoes. We also note that most of the brightening occurs between the second and third epochs in a 9 month time-span, indicating that the peak was at some time between these epochs.

We conclude that there are three remaining eruption scenarios to which our observed light curve could be assigned: 1) the 1838 peak, 2) the 1843 peak, and 3) the 1845 peak. A fourth possibility is an even earlier, unrecorded brightening. Our ability to decide among the different scenarios relies on the time differences between our images and spectra. The second- and third-epoch pair have only 9 months between them and therefore provide strong discrimination for brightenings. The spectroscopic observations were done shortly after the third-epoch images, corresponding to $<$9 months after a brightness maximum.

We now discuss the individual scenarios and the likelihood that they correspond to the brightening observed in our images:

- **1838 peak:** The first two epochs agree very well with the historical light curve. The historical light curve seems to decline faster after the peak at the beginning of 1838. Unfortunately, the historical data that constrain this decline are few and have large uncertainties. In addition, if the width of the scattering dust filament is very large, then the window function can span a wide range of epochs, which would cause the light-echo light curve to have a shallower decline then the event light curve.

- **1843 peak:** The first two epochs again agree very well. The decline in brightness is in very good agreement with what would be expected from the historical light curve.

- **1845 peak:** The first two epochs also agree very well with the 1845 peak. However, the current decline in brightness ($\approx$0.6 mag yr^{-1}) is considerably faster than the typical decline of $\approx$0.1mag yr^{-1} observed after 1845. The light-echo light curve can only be put in agreement with the historical light curve if there was a fast, unobserved decline from the peak in 1845.

We conclude that the most likely source of the light echoes for which we have spectra is the 1843 outburst, shortly after its peak. Assuming typical dust properties as observed for light echoes of other Galactic sources [16], the spectra is the light-curve-weighted average over an epoch range of 1-4 months. In the future, we will be able to further constrain the epoch range with additional imaging data. The two peaks in 1838 and 1845 cannot yet be excluded completely, but continued observations of the light echoes at monthly intervals should discriminate the possibilities within a year. This work, combined with targeted new observations and other contemporary images which may become known, will likely provide a detailed photometric time-series of the Great

Eruption with the probability of a useful companion spectral time-series. The recovery of valuable astrophysical observational data from the pre-imaging era is another powerful illustration of the power of light-echo observations

Name	UT Date	Telescope	Instrument	Exptime (sec)	Grism (lines/mm)	Slitwidth ($''$)	Range (Å)	FWHM resolution (Å)	P. A. (deg)	Observer
EC1A	2011/04/06	Magellan I 6.5m	IMACS	2×1800	300	0.9	$3800 - 10000$	4	339	J. Prieto
EC1B	2011/03/07	Magellan I 6.5m	IMACS	2×1800	200	0.9	$4000 - 10000$	8	324	R. Chornock & R. Foley
EC1C	2011/04/08	du Pont 2.5m	WFCCD	5×1800	400	1.7	$3700 - 9200$	7	339	J. Prieto

Table S1: Supplementary Information: Log of Spectroscopic Observations

Star Name	HD	Spectral Type	$T_{\rm eff}$
N Car	HD 47306	A0 II	9500
HR 4541	HD 102878	A2 Iab	9100
...	HD 34295	A4 II	8800
n Vel	HD 74272	A5 II	8500
y Car	HD 97534	A6 Ia	8400
HR 3739	HD 81471	A7 Iab	8300
ι Car	HD 80404	A8 Ib	8200
...	HD 104111	A8 II	8200
V399 Car	HD 90772	A9 Ia	8000
HR 3496	HD 75276	F2 Iab	7480
b Vel	HD 74180	F3 Ia	7320
HR 5024	HD 115778	F4 II	7160
ρ Pup	HD 67523	F6 II	6600
BG Cru	HD 108968	F7 Ib/II	6400
HR 8470	HD 210848	F7 II	6400
δ CMa	HD 54605	F8 Iab	6200
V810 Cen	HD 101947	F9 Iab	5900
γ^1 Nor	HD 146143	F9 Ia	5900
BB Sgr	HD 174383	G0 Ib	5500
ER Car	HD 97082	G1 Iab/Ib	5300
...	HD 136537	G2 II	5100
β Crv	HD 109379	G5 II	4830
...	HD 125809	G5/G6 Ib	4790
HR 3673	HD 79698	G6 II	4750
τ Leo	HD 99648	G8 Iab	4590
d Cen	HD 117440	G9 Ib	4500
HR 3583	HD 77020	G9 II	4500
HR 554	HD 11643	K1 II	4400
ϵ Peg	HD 206778	K2 Ib	4300
3 Cet	HD 225212	K3 Iab	4000
HR 611	HD 12642	K5 Iab	3750
HR 2508	HD 49331	M1 Iab	3450
V528 Car	HD 95950	M2 Ib	3350
CR Cir	HD 131217	M2/M3 II	3300

Table S2: Supplementary Information: UVES Supergiant Stellar Spectra Library[17]. We convert the spectral type into the effective temperature $T_{\rm eff}$ using the spectral-type to temperature relation for supergiants [30]

Star Name	HD	Spectral Type	T_0	$T_{\rm eff}$
5 Per	HD 13267	B5 Ia	13800	13700
ν Cep	HD 207260	A2 Ia	9100	9100
ϕ Cas	HD 7927	F0 Ia	7425	7800
ν Aql	HD 182835	F2 Ib	7350	7480
44 Cyg	HD 195593	F5 Iab	6600	7000
35 Cyg	HD 193370	F6 Ib	6200	6600
V440 Per	HD 14662	F7 Ib	5900	6400
HR 7008	HD 172365	F8 Ib-II	5500	6200
...	HD 18391	G0 Ia	5500	5500
HR 7456	HD 185018	G0 Ib	5550	5500
14 Per	HD 16901	G0 Ib-II	5478	5500
HR 3459	HD 74395	G2 Iab	5250	5100
β Dra	HD 159181	G2 Iab	5250	5100
...	HD 187299	G5 Ia	5010	4830
β Lep	HD 36079	G5 II	5170	4830
ξ Pup	HD 63700	G6 Ia	4990	4750
ξ^1 Cet	HD 13611	G8 Iab	5040	4590
...	HD 12014	K0 Ib	5173	4450
ζ Cep	HD 210745	K1.5 Ib	4500	4350
γ^1 And	HD 12533	K3 IIb	4383	4000
41 Gem	HD 52005	K4 Iab	4116	3900
V809 Cas	HD 219978	K4.5 Ib	4250	3825
α Ori	HD 39801	M2 Iab	3614	3350

Table S3: Supplementary Information: Ca II IR triplet Supergiant Stellar Spectra Library[18]. The temperature T_0 is the effective temperature quoted by Cenarro et al.[18]. For consistency we also calculate $T_{\rm eff}$ using the same stellar type-temperature relation[30] we used for the UVES spectral library.

Line	λ_{min}	λ_{max}
O I 5577.4	5572	5582
Na I D 5890.0, 5895.9	5860	5921
O I 6300.2	6295	6305
O I 6363.9	6359	6369

Table S4: List of the fore/background emission lines which are excluded from the 5050-6500 Åwavelength range of the correlation analysis. For each spectroscopic line, λ_{min} and λ_{max} define the initial and final wavelengths in Å of the contaminating line region we exclude.

	03/03/2011	05/10/2010	02/06/2011	03/08/2011	03/24/2011	05/14/2011	05/25/2011	07/01/2011	07/27/2011
Instrument	CTIO4m Mosaic II	CTIO4m Mosaic II	CTIO4m Mosaic II	Magellan IMACS f2	FTS	FTS	FTS	CTIO4m Mosaic II	FTS
MJD	52708.11960	55326.01102	55598.22252	55628.26319	55644.39484	55695.38567	55706.41416	55743.98288	55769.35728
Exp. time	60	120	120	30	600	1200	600	120	600
F0	1.40 ± 0.13	...	6.86 ± 0.19	6.82 ± 0.21	6.95 ± 0.21	6.22 ± 0.18	6.15 ± 0.19	5.66 ± 0.18	5.67 ± 0.21
F1	1.02 ± 0.11	...	7.45 ± 0.17	7.20 ± 0.18	6.85 ± 0.18	6.16 ± 0.16	6.13 ± 0.17	5.45 ± 0.15	5.10 ± 0.18
F2	1.27 ± 0.11	...	7.39 ± 0.16	6.92 ± 0.17	6.88 ± 0.17	6.14 ± 0.15	6.10 ± 0.16	5.62 ± 0.15	5.26 ± 0.17
F3	1.32 ± 0.11	...	7.32 ± 0.16	6.86 ± 0.18	6.86 ± 0.18	6.04 ± 0.15	6.09 ± 0.16	5.76 ± 0.15	5.42 ± 0.18
F4	1.22 ± 0.11	...	7.27 ± 0.16	7.00 ± 0.18	6.93 ± 0.18	6.16 ± 0.15	6.08 ± 0.16	5.58 ± 0.15	5.37 ± 0.18
F5	1.39 ± 0.10	...	7.26 ± 0.15	6.93 ± 0.16	6.84 ± 0.16	6.10 ± 0.14	6.12 ± 0.15	5.58 ± 0.14	5.54 ± 0.16
F6	1.38 ± 0.09	...	7.31 ± 0.13	7.31 ± 0.13	7.06 ± 0.14	6.06 ± 0.12	5.97 ± 0.12	5.57 ± 0.12	5.17 ± 0.13
F7	1.36 ± 0.08	...	7.15 ± 0.12	6.98 ± 0.13	6.80 ± 0.13	6.13 ± 0.11	6.09 ± 0.12	5.85 ± 0.11	5.34 ± 0.13
F8	1.06 ± 0.09	...	6.66 ± 0.13	6.64 ± 0.14	6.95 ± 0.14	6.21 ± 0.12	6.14 ± 0.13	5.90 ± 0.12	5.82 ± 0.14
F9	1.07 ± 0.09	...	6.61 ± 0.13	6.87 ± 0.14	6.94 ± 0.14	6.25 ± 0.12	6.14 ± 0.13	5.93 ± 0.12	5.60 ± 0.14
F10	1.13 ± 0.08	...	6.58 ± 0.12	7.00 ± 0.13	7.04 ± 0.13	6.30 ± 0.11	6.25 ± 0.12	5.78 ± 0.11	5.41 ± 0.13
F11	1.13 ± 0.08	...	6.98 ± 0.11	7.32 ± 0.13	6.98 ± 0.12	6.28 ± 0.11	6.00 ± 0.11	5.67 ± 0.11	5.23 ± 0.12
F12	1.27 ± 0.08	2.61 ± 0.16	6.95 ± 0.11	7.56 ± 0.12	7.04 ± 0.12	6.15 ± 0.11	5.92 ± 0.11	5.68 ± 0.11	5.21 ± 0.12
F13	1.43 ± 0.09	2.65 ± 0.12	6.93 ± 0.12	7.40 ± 0.14	6.90 ± 0.13	6.05 ± 0.12	6.02 ± 0.12	5.83 ± 0.11	5.32 ± 0.13
$\bar{F}$	1.24	2.64	7.01	7.09	6.94	6.17	6.08	5.72	5.38
$\sigma_{\bar{F}}$	0.14	0.02	0.29	0.25	0.08	0.08	0.08	0.14	0.20

Table S5: The individual lightcurves are normalized so that the average $-2.5\log_{10}(F) = -2.0$ for MJD in 55590-555660. For the image from 05/10/2010, 12 out of 14 positions fell into the chip gap and could not be determined.

1. Davidson, K. & Humphreys, R. M. Eta Carinae and Its Environment. Annu. Rev. Astron. Astr. **35**, 1–32 (1997).

2. Damineli, A. The 5.52 Year Cycle of Eta Carinae. Astrophys. J. **460**, L49+ (1996).

3. Smith, N. The Structure of the Homunculus. I. Shape and Latitude Dependence from H_2 and [Fe II] Velocity Maps of η Carinae. Astrophys. J. **644**, 1151–1163 (2006).

4. Smith, N. & Frew, D. J. A revised historical light curve of Eta Carinae and the timing of close periastron encounters. Mon. Not. R. Astron. Soc. 1097–+ (2011).

5. Smith, N. *et al.* Mass and Kinetic Energy of the Homunculus Nebula around η Carinae. Astron. J. **125**, 1458–1466 (2003).

6. Smith, N. A blast wave from the 1843 eruption of ϵ Carinae. Nature **455**, 201–203 (2008).

7. Goodrich, R. W., Stringfellow, G. S., Penrod, G. D. & Filippenko, A. V. SN 1961V - an extragalactic ETA Carinae analog. Astrophys. J. **342**, 908–916 (1989).

8. Humphreys, R. M. & Davidson, K. The luminous blue variables: Astrophysical geysers. Publ. Astron. Soc. Pac. **106**, 1025–1051 (1994).

9. Humphreys, R. M., Davidson, K. & Smith, N. Eta Carinae's Second Eruption and the Light Curves of the eta Carinae Variables. Publ. Astron. Soc. Pac. **111**, 1124–1131 (1999).

10. Van Dyk, S. D. *et al.* SN 1997bs in M66: Another Extragalactic η Carinae Analog? Publ. Astron. Soc. Pac. **112**, 1532–1541 (2000). arXiv:astro-ph/0009027.

11. Vink, J. S. Eta Carinae and the Luminous Blue Variables. *ArXiv e-prints* (2009). 0905.3338.

12. Kashi, A., Frankowski, A. & Soker, N. NGC 300 OT2008-1 as a Scaled-down Version of the Eta Carinae Great Eruption. Astrophys. J. **709**, L11–L15 (2010).

13. Smith, N., Li, W., Silverman, J. M., Ganeshalingam, M. & Filippenko, A. V. Luminous blue variable eruptions and related transients: diversity of progenitors and outburst properties. Mon. Not. R. Astron. Soc. **415**, 773–810 (2011).

14. Rest, A. *et al.* Light echoes from ancient supernovae in the Large Magellanic Cloud. Nature **438**, 1132–1134 (2005).

15. Rest, A. *et al.* Scattered-Light Echoes from the Historical Galactic Supernovae Cassiopeia A and Tycho (SN 1572). Astrophys. J. **681**, L81–L84 (2008).

16. Rest, A. *et al.* On the Interpretation of Supernova Light Echo Profiles and Spectra. Astrophys. J. **732**, 2–+ (2011).

17. Bagnulo, S. *et al.* The UVES Paranal Observatory Project: A Library of High- Resolution Spectra of Stars across the Hertzsprung-Russell Diagram. *The Messenger* **114**, 10–14 (2003).

18. Cenarro, A. J. *et al.* Empirical calibration of the near-infrared Ca ii triplet - I. The stellar library and index definition. Mon. Not. R. Astron. Soc. **326**, 959–980 (2001).

19. Smith, N., Vink, J. S. & de Koter, A. The Missing Luminous Blue Variables and the Bistability Jump. Astrophys. J. **615**, 475–484 (2004).

20. Davidson, K. The relation between apparent temperature and mass-loss rate in hypergiant eruptions. Astrophys. J. **317**, 760–764 (1987).

21. Le Sueur, A. On the Nebulae of Argo and Orion, and on the Spectrum of Jupiter. *Royal Society of London Proceedings Series I* **18**, 245–250 (1869).

22. Le Sueur, A. Observations with the Great Melbourne Telescope, in a Letter to Prof. Stokes. *Royal Society of London Proceedings Series I* **19**, 18–19 (1870).

23. Walborn, N. R. & Liller, M. H. The earliest spectroscopic observations of eta Carinae and its interaction with the Carina Nebula. Astrophys. J. **211**, 181–183 (1977).

24. Humphreys, R. M., Davidson, K. & Koppelman, M. The Early Spectra of Eta Carinae 1892 to 1941 and the Onset of its High Excitation Emission Spectrum. Astron. J. **135**, 1249–1263 (2008).

25. Smith, N. Doppler tomography of the Little Homunculus: high-resolution spectra of [FeII]λ16435 around Eta Carinae*. Mon. Not. R. Astron. Soc. **357**, 1330–1336 (2005).

26. Smith, N. *et al.* Discovery of Precursor Luminous Blue Variable Outbursts in Two Recent Optical Transients: The Fitfully Variable Missing Links UGC 2773-OT and SN 2009ip. Astron. J. **139**, 1451–1467 (2010).

27. Foley, R. J. *et al.* The Diversity of Massive Star Outbursts. I. Observations of SN2009ip, UGC 2773 OT2009-1, and Their Progenitors . Astrophys. J. **732**, 32–+ (2011).

28. Frew, D. J. The Historical Record of η Carinae I. The Visual Light Curve, 1595-2000. *Journal of Astronomical Data* **10**, 6–+ (2004).

29. Walborn, N. R., Danks, A. C., Vieira, G. & Landsman, W. B. Space Telescope Imaging Spectrograph Observations of High-Velocity Interstellar Absorption-Line Profiles in the Carina Nebula. Astrophys. J. Sup. **140**, 407–456 (2002).

30. Humphreys, R. M. & McElroy, D. B. The initial mass function for massive stars in the Galaxy and the Magellanic Clouds. Astrophys. J. **284**, 565–577 (1984).

31. Couderc, P. Les auréoles lumineuses des Novae. *Annales d'Astrophysique* **2**, 271 (1939).

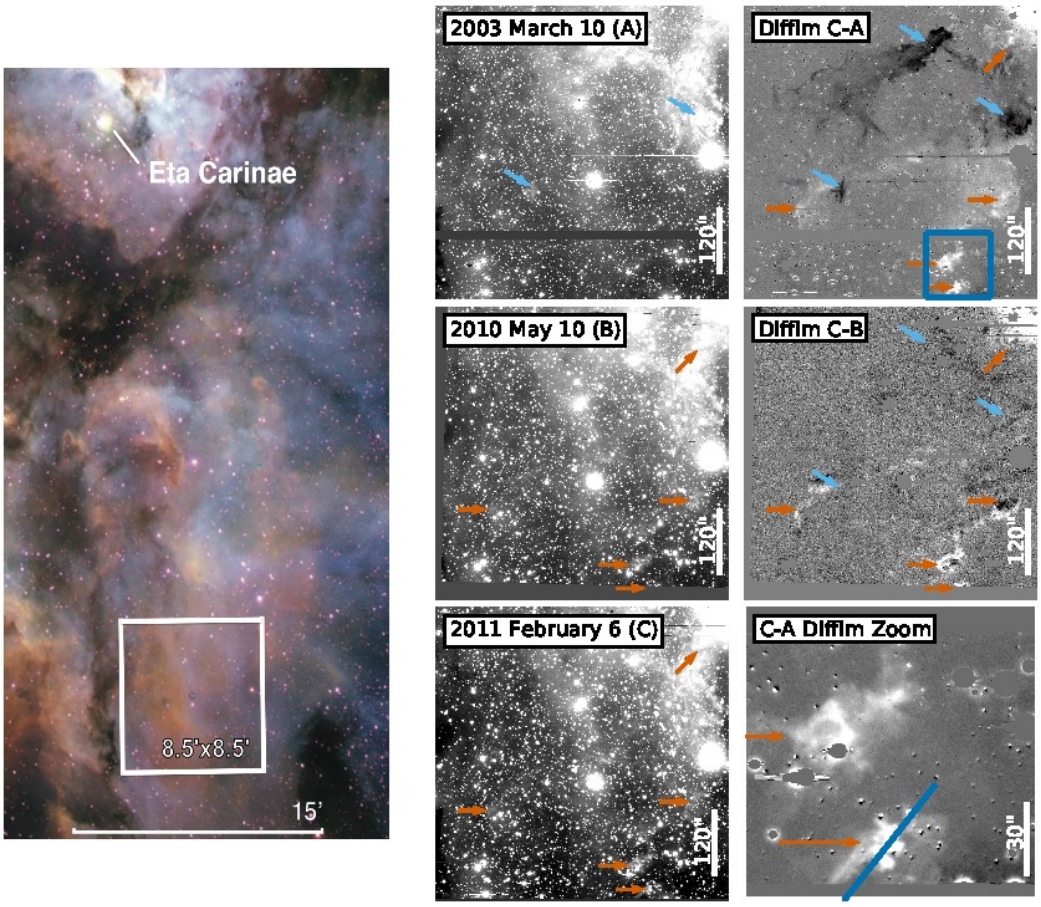

Figure 1

η Car light echoes. The left panel shows the positions of η Car and our images (white box), plotted on an image in the light of 3 different emission lines: oxygen (blue), hydrogen (green), and sulfur (red) (credit: Nathan Smith, University of Arizona/NOAO/AURA/NSF). The middle panels show the images at epochs 2003 March 10 (A), 2010 May 10 (B), and 2011 Feb 6 (C), from top to bottom. The right panels show the difference images C-A and C-B at the top and middle, respectively. Example light-echo positions are indicated with blue (epoch A) and red (epoch B and C) arrows. The bottom right panel shows a zoom of the spectrograph slit, indicated with a blue line. For all panels north is up and east is to the left.

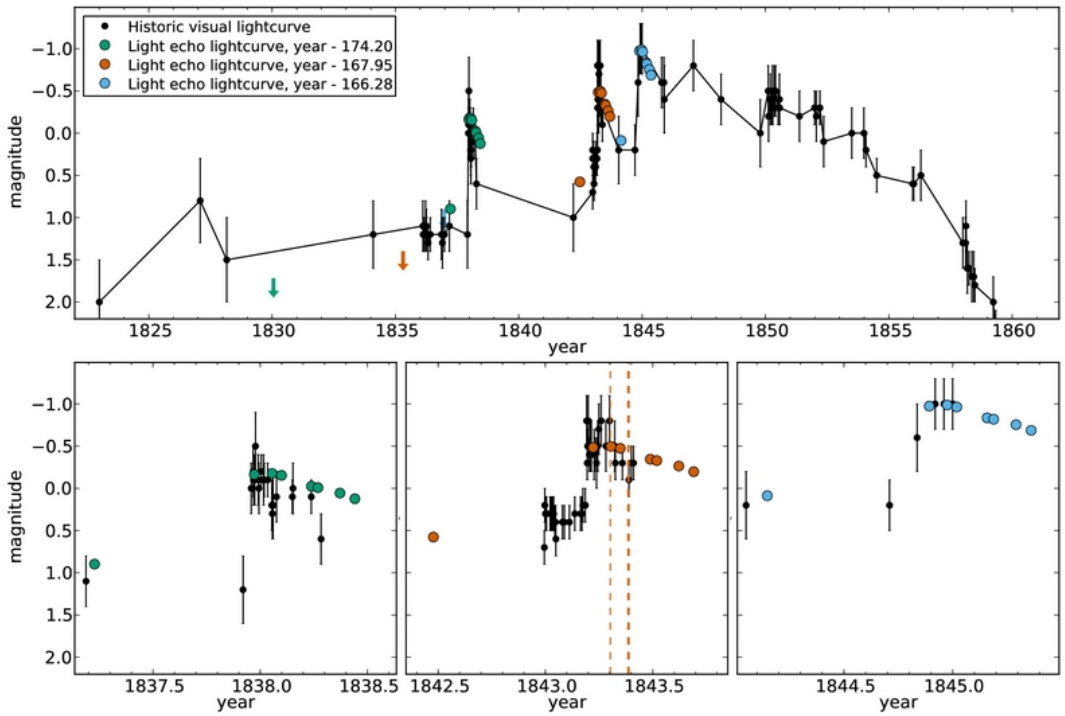

Figure 2

Comparison between the historical light curve in visual apparent magnitudes (black circles and black line), and the recovered light-echo light curves (SDSS i) derived in this work. Brightnesses from our eight modern images spanning $\sim$8 years are displayed shifted by 174.2 yrs (green circles), 167.95 yrs (red circles), and 166.28 yrs (blue circles), in order to illustrate the best-matching time delays for the 1838, 1843, and 1845 outbursts, respectively. The first epoch is an upper limit indicated with an arrow. The upper panel shows the full time range of the Great Eruption and therefore shows all three potential matches, whereas the lower panels show the brightnesses from seven of our eight modern epochs in a magnified time period around each peak.

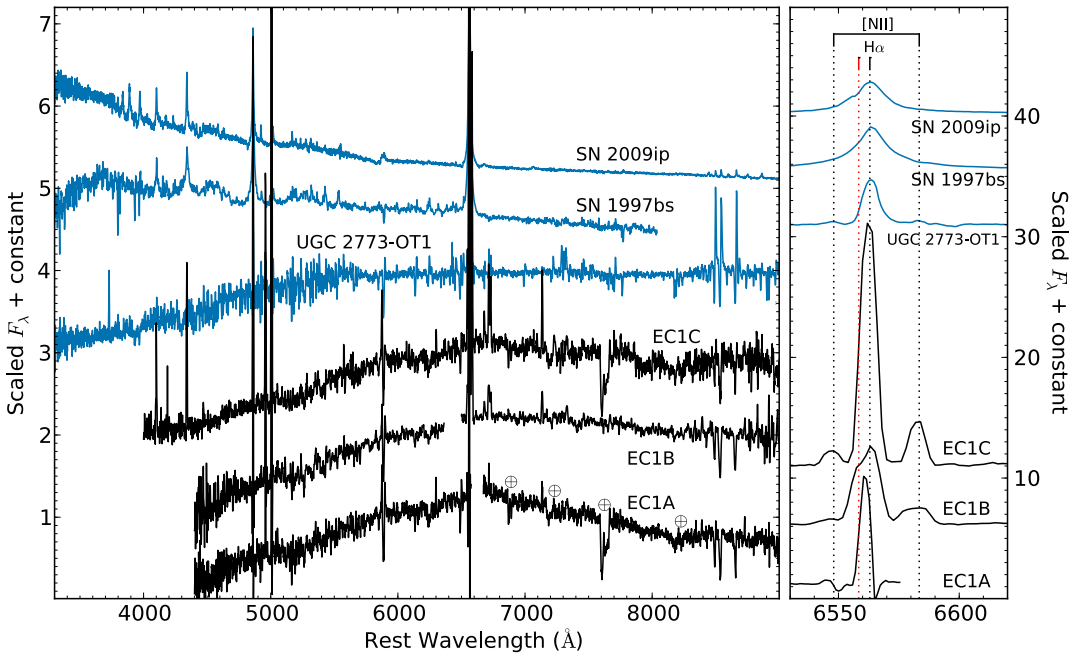

Figure 3

Three optical low-resolution spectra of the light echo (black lines). They were taken at J2000 position RA=10:44:12.127 and Decl.=−60:16:01.69 in March and April 2011 obtained at the Magellan I 6.5-m and du Pont 2.5-m telescopes of the Las Campanas Observatory, Chile. A log of the spectroscopic observations and details of the spectra is presented in Table S1. The spectra were reduced using standard techniques and then wavelength-calibrated using observations of an HeNeAr lamp. The wavelength calibration was checked and corrected using night-sky emission lines, especially O I 5577Å, and OH lines in the red part of the spectrum. We flux-calibrated the spectra using a flux standard observed the same night as the science observations. The left panel shows the spectra from 5000 to 9000Å. The spectra are not corrected for reddening nor for the blue-ward scattering by the dust. The blue lines show for comparison spectra of three examples of SN impostors: SN 1997bs, SN 2009ip, and UGC 2773-OT1. The right panel shows the Hα and [N II] emission lines. Note that the background emission-line subtraction is incomplete since they spatially vary. Also, for EC1A Hα is at the edge of the chip and is therefore uncertain.

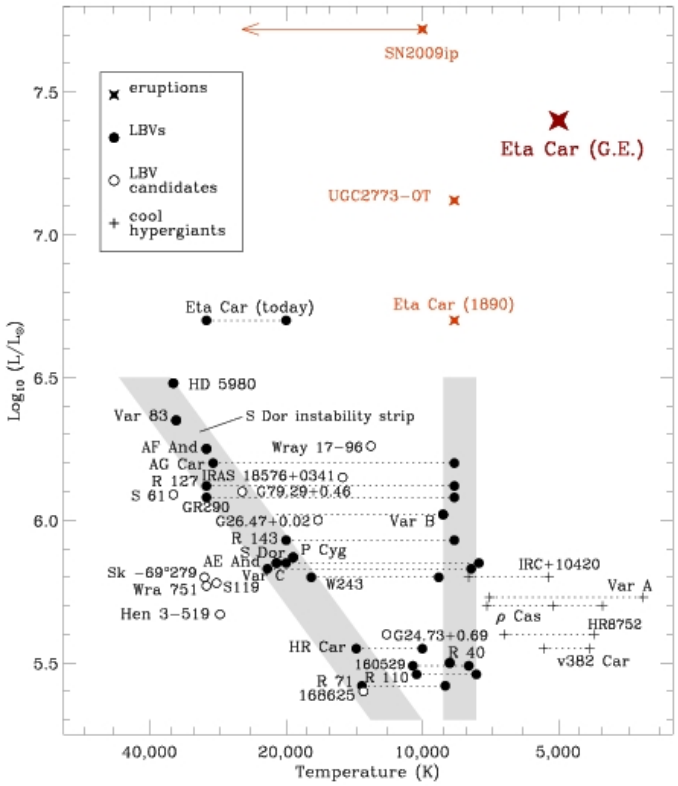

Figure 4 Adaptation[19] of an HR diagram with LBVs, related hypergiant stars, and the peak luminosities of LBV-like eruptions. The grey bands denote the typical locations of LBVs in quiescence and in S Doradus excursions. Temperatures for the Great Eruption and 1890 eruption of η Car are based on the echo spectra presented here and the F-type spectrum of the 1890 event[23], respectively. The temperature of 10,000 K for SN 2009ip is based on the observed continuum shape, but this is only a lower limit because of the possible effects of circumstellar or host galaxy reddening[26]. Because of the presence of He I lines in the spectrum, the true temperature is probably much hotter. The 8500 K temperature of UGC2773-OT is indicated by the F-type absorption features in its spectrum, and this temperature is relatively independent of reddening[26,27].

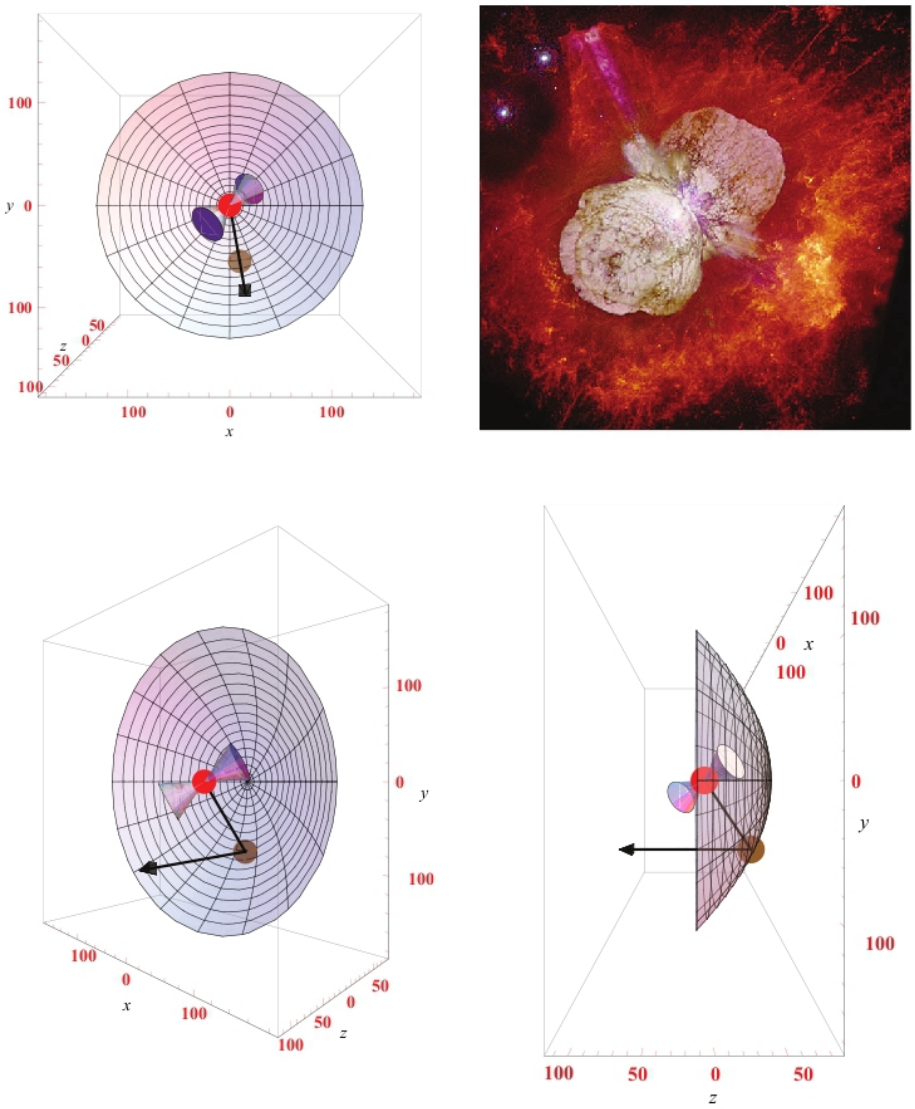

Figure 5
3D-plot of the light path. North is toward the positive y-axis (up), east is toward the negative x-axis (left), and the positive z-axis points toward the observer with the origin at η Car. The red and brown circles indicate η Car and scattering dust, respectively. The parabolic relation between the spatial parameters of the scattering dust and the time since outburst is described by the well-known light echo equation[31]: Assuming a time since outburst of 169 years, and a distance of 7660 light-years[3], we find that the scattering dust is at a position (x,y,z)=(14,-78,-66) in light-years. The black lines show the path of the light scattering from the light-echo-producing dust concentrations. The top-right panel shows an *HST* image (credit: Nathan Smith / Jon Morse / NASA) of η Car, which is surrounded by expanding lobes of gas denoted as the Homunculus Nebula visible to the NW and SE. These lobes were created by the 1838-1858 Great Eruption. We indicate the lobes in the 3D plots with the two cones (Note that the size of the cones is not to scale).

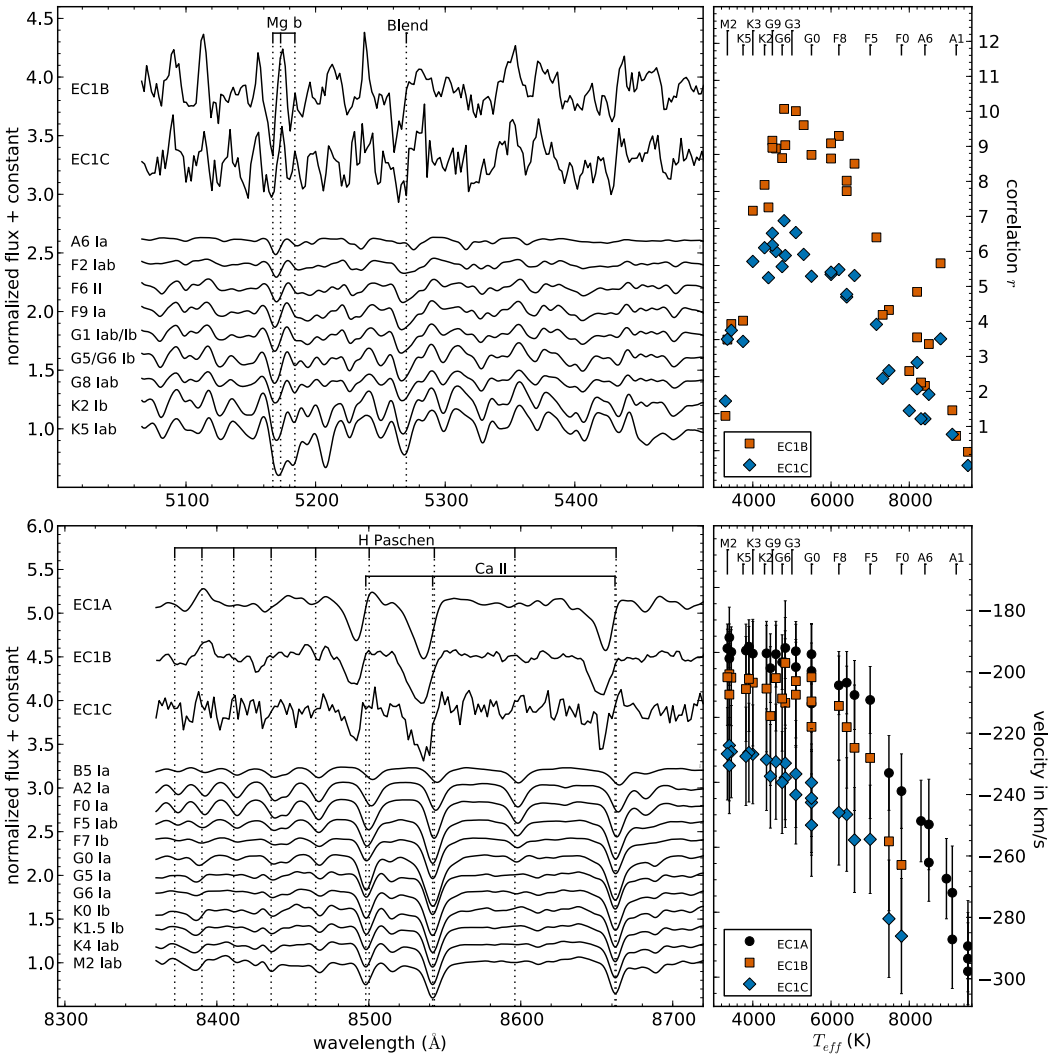

Figure 6

Spectral type comparison. The stellar comparison spectra are convolved with a Gaussian of FWHM 7 Å so that their resolution matches those of EC1B and EC1C. Similarly, we convolve the spectrum EC1A, which has an original resolution of 4Å, with a Gaussian of FWHM 5.7 Å. We then divide the spectra by the low-order continuum which we determine by convolving the spectra with a Gaussian of FWHM 200 Å. The upper left panel compares two of the observed light echo spectra to a selection of UVES supergiants[17] in the 5060-5500 Å wavelength range (We do not show spectrum EC1A since its S/N ratio in this blue wavelength range is too low). The light echo spectra correlate very well with late-F and G-type stars, in particular the Mg b lines, and the Ca I, Fe I, Ti I, Cr I blend at 5270 Å. The upper right panel shows the cross-correlation between the light echo and the UVES spectra in the wavelength range of 5050-6500 Å as calculated by the IRAF routine `xcsao`. Since the UVES spectra have a gap around the Ca II IR triplet, we use the Ca II triplet spectral library[18] in that wavelength range, as shown in the bottom left panel. The bottom right panel shows the blue-shifted velocity determined by `xcsao` from the Ca II triplet with respect to the effective temperature[30] of the supergiant template spectra.

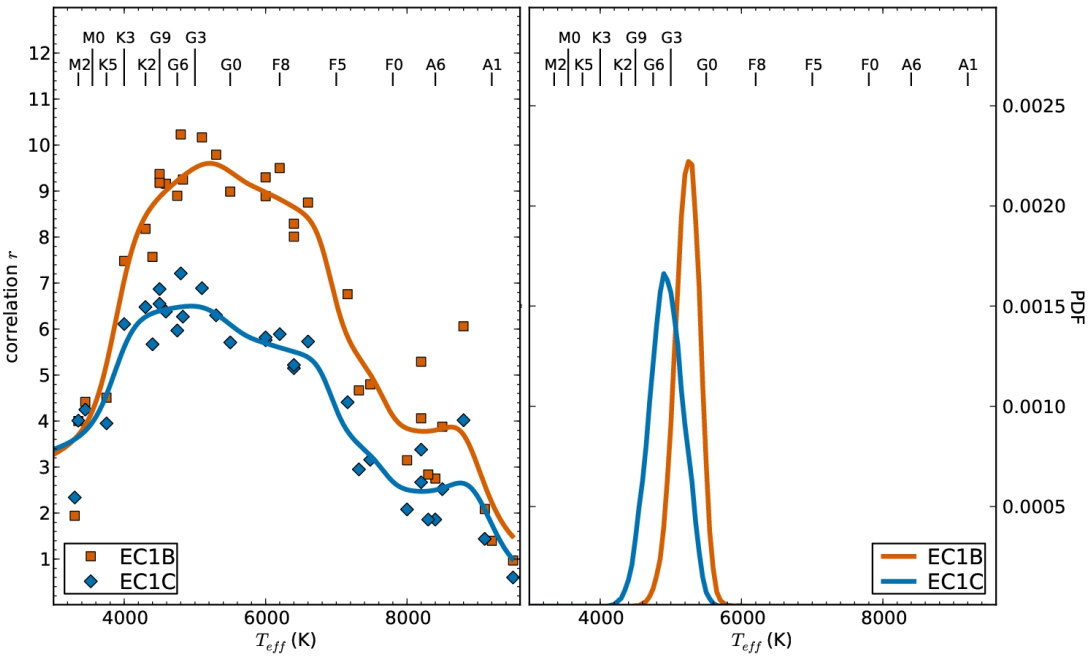

Figure 7

The left panel shows the cross-correlation between the light echo and the UVES spectra as calculated by the IRAF routine `xcsao` for EC1B (red squares) and EC1C (blue diamonds). The lines indicate $r(T)$ smoothed with a Gaussian of width $\sigma = 300$ K, peaking at 5210 K and 4950 K for EC1B (red) and EC1C (blue), respectively. The right panel shows the PDF of the best-correlating supergiant temperature, determined by bootstrap resampling the r distribution 10^5 times. The 95% temperature confidence intervals are 4850-5550 K and 4450-5400 K for EC1B and EC1C, respectively.